Journal of MATERIALS RESEARCH

Invited Review
DOI: 10.1557/jmr.2018.429

This section of Journal of Materials Research is reserved for papers that are reviews of literature in a given area.

FOCUS ISSUE

UNDERSTANDING WATER-OXIDE INTERFACES TO HARNESS NEW PROCESSES AND TECHNOLOGIES

Thin water films covering oxide nanomaterials: Stability issues and influences on materials processing

Gilles R. Bourret[1] Oliver Diwald[1,a)]

[1]*Department of Chemistry and Physics of Materials, Paris Lodron University of Salzburg, Salzburg A-5020, Austria*
[a)]Address all correspondence to this author. e-mail: oliver.diwald@sbg.ac.at

Received: 31 July 2018; accepted: 23 October 2018

Ambient water condenses readily on metal oxides, which can lead to water film formation and water-mediated reactions at the oxide surface. Similar to bulk water, thin water films with thicknesses below 10 molecular layers can modify the oxide surface chemical reactivity and stability. However, due to the confinement of mass transport at the oxide surface, these processes do not proceed exactly as they do in bulk liquid water. In this review article, we will present selected examples from our group and others' that illustrate the rich interaction of MgO and TiO_2 nanostructures with thin water films. We will show that these condensed water films can induce significant chemical, structural, and microstructural transformations of metal oxide nanostructures such as dissolution/precipitation, morphological changes, crystallization, and self-assembly in the solid state.

Introduction

Water is ubiquitous under ambient conditions and condenses readily at metal oxide surfaces. Water adsorption, water film formation, and water-mediated reactions on metal oxide surfaces are therefore fundamentally important in environmental chemistry, in catalysis, and for processing of functional metal oxides in general [1]. During materials operation under ambient conditions, thin films of mostly undefined composition and structure cover the metal oxide nanoparticle surfaces. Therefore, the boundaries between oxide nanoparticles and the environmental phase need to be described as interfaces rather than as surfaces. Similar to bulk water, such thin water films alter the oxide surface by modifying its chemical reactivity and stability [2, 3, 4, 5, 6, 7, 8, 9]. This can lead to chemical, structural, and microstructural transformations such as dissolution/precipitation, morphological changes, crystallization, high-index facet stabilization [10, 11], or self-assembly (Fig. 1) [12, 13, 14]. However, due to the confinement of mass transport at the oxide surface, these processes do not proceed exactly as they do in bulk liquid water.

In this review, we will present selected examples from our group and others' that studied water thin film–mediated transformations of well-defined metal oxide nanostructures. We focus on MgO and TiO_2 nanostructures that are canonical metal oxide model systems and have been extensively studied for decades [15, 16, 17, 18]. In addition to their importance for ceramics, both metal oxides have been widely used as model systems for surface science studies and modelling. Whereas MgO is a strongly ionic metal oxide that crystallizes in the simple rock salt structure and exhibits enhanced solubility in nanoparticulate form, TiO_2 is a transition metal oxide with substantial amount of covalent bonding, which, even as a nanocrystalline materials, shows almost no solubility at room temperature.

Additionally, our group has become expert in the synthesis of surfactant-free single-crystalline MgO nanocubes, which are well suited for fundamental studies due to their structural and compositional purity. They are, therefore, great substrates for such investigations and will be presented in section Vapor phase–grown MgO nanoparticles. Through this review article, we would like to introduce the reader to the rich and various ways water thin films can alter metal oxide particle structure, morphology, and composition. We will introduce water thin film formation on metal oxides (section Water thin film on metal oxides), followed by discussing its use to confine chemical reactions (section Thin water films as a two-dimensional solvent for enhanced chemical growth) and its influence on metal oxide nanostructure stability (section Residual water and transformations of metal oxide nanoparticles in high vacuum). The use of hydroxylated surfaces to drive nanostructure self-assembly in the

https://doi.org/10.1557/jmr.2018.429 Published online by Cambridge University Press

© Materials Research Society 2019

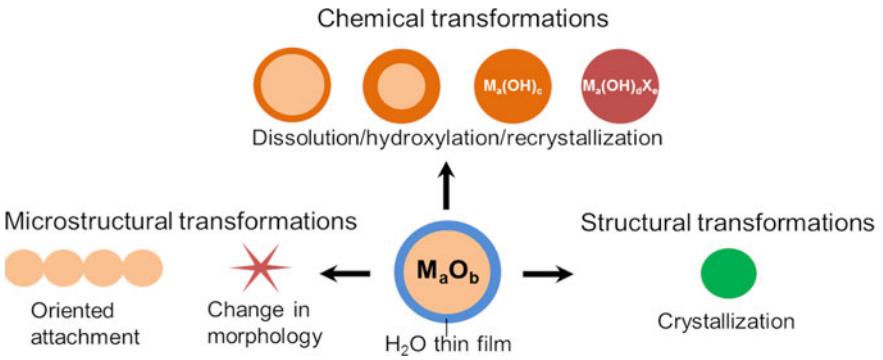


Figure 1: The possible effects of thin water films on metal oxide nanostructure composition, structure, and morphology.

solid state will then be discussed (section Self-assembly processes in thin water films). We will follow by presenting recent results on water thin film mediated sintering and crystallization processes at elevated temperatures (section Impact of adsorbed water on materials transformation at elevated temperatures). Finally, we will compare the effect of water vapor and liquid water on the stability of metal oxide nanostructures (section Metal oxide immersion into condensed water) and conclude with an outlook on this understudied and exciting field of research (section Concluding remarks and perspectives).

Metal oxide nanoparticles and thin water films

Vapor phase–grown MgO nanoparticles

The MgO nanoparticle cubes described in this review were synthesized by combustion reactions and ranged in size between 1 and 1000 nm. The absence of solvents during nucleation and growth prevented substantial particle aggregation and sintering. In the past, it has been demonstrated that this material represents a well-suited model system for surface science studies that aim at bridging the information gap between atomic level understanding on ordered MgO single crystal surfaces [19, 20] and metal oxide particle powders as technologically relevant materials components. Two particle systems were used: polydisperse MgO cubes, which were collected by Mg combustion in air [15, 21, 22, 23, 24], with sizes ranging from 1 to 1000 nm, and monodisperse MgO nanocubes synthesized by chemical vapor synthesis [18, 25] at reduced pressures exhibiting defined morphologies with an average edge length around 4 nm. As an additional prerequisite for studies on model systems, we annealed all particle powders in high vacuum as well as pure oxygen atmosphere in order to desorb and decompose adsorbed surface contaminants. These measures were taken to eliminate potential interferences of residual adsorbates with water adsorption and subsequent surface reactions.

Despite the growing number of publications on oxide nanocrystals—predominantly on colloidal particle systems—that address the geometrical shape of crystalline polyhedra and that deal with the estimation of relative and absolute surface areas of different crystal facets, there are only rare cases of nanoparticle systems that have clean particle surfaces and well-defined particle morphologies at the same time. Vapor phase synthesis of metal oxide nanoparticles has the principal advantage to provide materials of high purity and, therefore, of better defined surface compositions than liquid phase synthesis [18].

Water thin film on metal oxides

Adsorption and adsorption-induced chemical processes that occur at the metal oxide–water vapor or metal oxide–liquid water interfaces are typically accompanied by microstructural changes of nanoparticle ensembles [26, 27]. Despite their great importance for materials science and in particular for the stability of oxide nanomaterials, the initial reactions of water vapor with solid oxide substrates (e.g., the processes of dissociative H_2O chemisorption versus H_2O physisorption), the thickness, and the structural properties of the thin liquid films are largely unexplored [6]. Thin water films under ambient conditions represent an intermediate case between liquid–solid and liquid–vapor interfaces that jointly determine its properties. For both natural and engineered nanomaterials, most solid surfaces in the ambient and at water partial pressures in the range between 1 and 30 Torr [Fig. 2(a)] are covered by several monolayers of water [Fig. 2(b)]. This was demonstrated for clean MgO (100) surfaces, which were investigated with FT-IR spectroscopy in atmospheres of variable relative humidity [28]. As shown in Fig. 2(b), at a relative humidity of 20% and above, a ~1–2 monolayer thick water layer already forms. In fact, hydroxylation and water adsorption start at a relative humidity (RH) <0.1% and significant amounts of molecular water become stabilized during the initial stages of water adsorption. Related observations underline the importance of OH–H_2O interaction, which is stronger than H_2O–H_2O bonds [6].

Surface science typically addresses water adsorption at the level of single molecules up to monolayer surface coverage. On

https://doi.org/10.1557/jmr.2018.429 Published online by Cambridge University Press

© Materials Research Society 2019

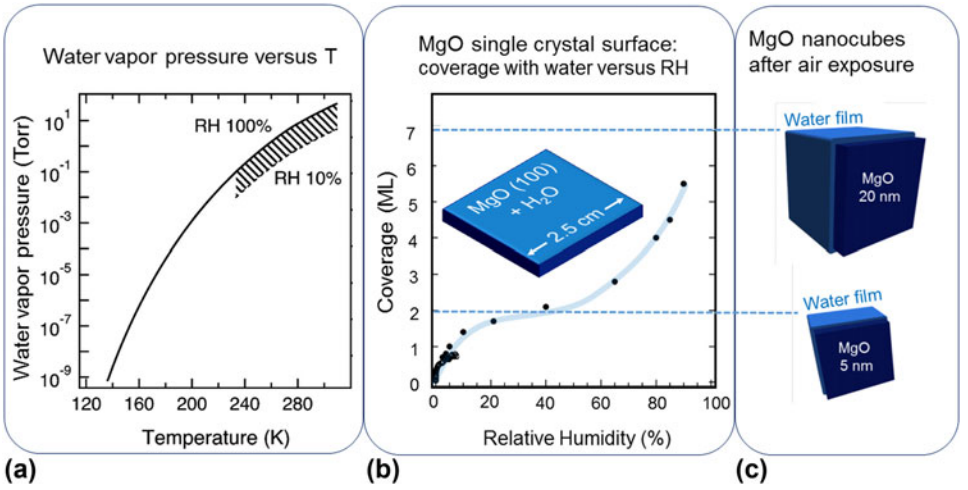


Figure 2: The composite plot underlines that the typical water vapor pressures present in air and at room temperature (a) lead to the instantaneous coverage of almost every oxide surface with water (b). In comparison with the results of a Fourier Transform Infrared (FT-IR) study, which was performed on clean MgO (100) single crystal surfaces [28], the significant H_2O uptake of MgO nanocube powders after 20 min of air exposure is demonstrated in (c). A weight increase of 20% measured for nanocube ensembles with edge lengths between 5 and 20 nm corresponds to the formation of water multilayers at the nanocube surface. Adapted with permission from Ref. 6 (Copyright 2016 American Chemical Society) and from Ref. 28 (Copyright 2005 Elsevier).

two-dimensional metal oxides, surface studies reveal that the structure of interfacial water, i.e., in the first hydration layers, is distinct from bulk water [29]. By means of in situ X-ray scattering techniques, it was found that the organization of hydration layers is limited to 1–2 nm, which corresponds to only a few water correlation lengths. For such hydration shell dimensions, related structures are highly dependent on characteristics of the metal oxide surface, such as local charge, spatial arrangement, and coordination of ions, and nature and abundance of additional adsorbates [30].

MgO nanocube powders with specific surface areas as large as 300 m^2/g represent a model system for adsorption studies on oxide nanomaterials [20, 31]. Previous temperature-programmed desorption measurements and thermogravimetric analysis revealed that—depending on the exposure time—the nanoparticle powder can adsorb water between 10 and 20% of weight. H_2O desorption features at $T = 303$ K and 573 K were observed and attributed to desorption of weakly bound surface water at $T = 303$ K and to the decomposition of surface $Mg(OH)_2$ [32] into MgO [33] and gas phase water at $T = 573$ K. An estimate for the number of water molecules per Mg^{2+}–O^{2-} surface unit as a function of MgO nanocube size reveals that the number of water layers can be between 2 and 7 monolayers for MgO nanocubes with sizes of 5 nm and 20 nm, respectively [Fig. 2(c)].

Thin water films as a two-dimensional solvent for enhanced chemical growth

Thin water films can act as a two-dimensional solvent and give rise to the spontaneous and spatially controllable growth of hydroxide fibers in ambient air and at room temperature [34, 35]. Gheisi et al. recently reported the formation of $Mg_3(OH)_5Cl{\cdot}4H_2O$ fibers on MgO nanocubes sequentially exposed to a $SiCl_4/O_2$ atmosphere at cryogenic temperatures and—in a subsequent step—to air or a water-saturated O_2 atmosphere. This remarkable transformation shows that water thin films promote reactions that are confined at the metal oxide surface (Fig. 3).

Residual water and transformations of metal oxide nanoparticles in high vacuum

Imaging of metal oxide particles with scanning electron microscope and helium ion microscope (HIM) requires powder sample immobilization on conductive substrates. This can be achieved by pressing the sample into a soft metal that, if not cleaned and prepared prior to sample immobilization, is typically covered with water originating from the ambient atmosphere. Under such conditions, residual and surface adsorbed water molecules can act as a solvent and lead to a partial conversion of MgO into $Mg(OH)_2$ [36]. HIM studies of MgO cubes obtained by Mg combustion (polydisperse sample with sizes ranging from 4 nm to a few micrometers) and pressed into an untreated indium foil have revealed that the samples prepared at the ambient and stored 4 days in high vacuum showed significant swelling, characteristic with a volume increase due to the formation of an $Mg(OH)_2$ shell. On the contrary, samples prepared using an indium foil that was dried in high vacuum (10^{-5} mbar, 1 day) before MgO cube immobilization showed very limited swelling. Interestingly and similar to the observations made in liquid water (see section Metal oxide immersion into condensed water), it was found that the smallest MgO cubes reacted faster than the larger ones, as shown by their larger relative swelling (in relation to their

https://doi.org/10.1557/jmr.2018.429 Published online by Cambridge University Press

© Materials Research Society 2019

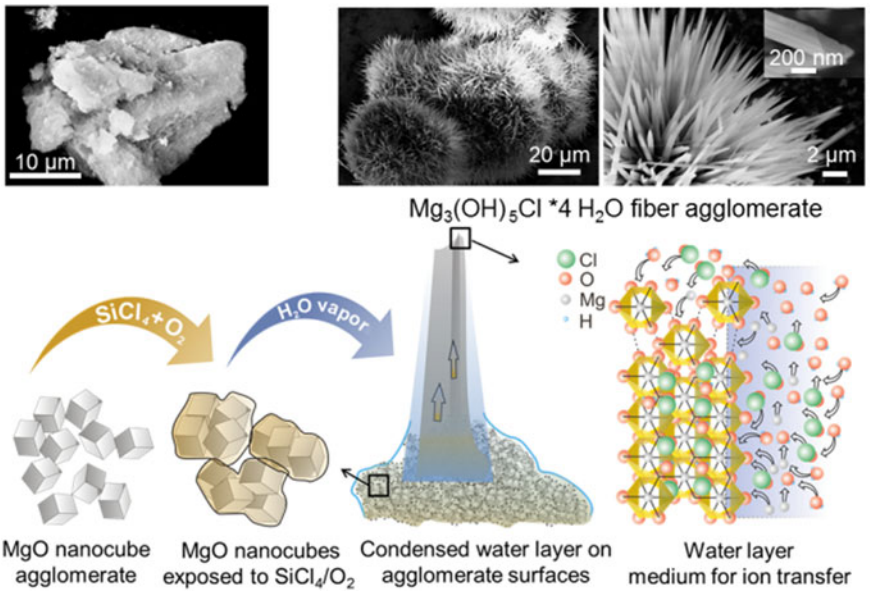


Figure 3: Thin water films covering highly dispersed metal oxides can give rise to the spontaneous and spatially controllable growth of hydroxide fibers out of the MgO nanocube agglomerates shown in the SEM image in the left upper panel. Surface chlorinated MgO nanocubes transform upon contact with water vapor at room temperature into magnesium hydroxychloride $Mg_3(OH)_5Cl{\cdot}4H_2O$ fibers. The formation of hydroxide fibers under ambient conditions can be applied to a variety of microstructural evolution processes that involve metastable solids and superficial water acting both as a reactant and as a reaction medium for the hydration of metal oxide particles. Figure adapted from [34, 35].

initial size). The fact that the ambient water condensed at the indium foil surface was sufficient to reactively attack the MgO cubes pressed into the foil and this under high vacuum conditions is remarkable [36]. It demonstrates that spurious amounts of water can react with metal nanostructures even under high vacuum conditions and should be taken into consideration by anyone working with water sensitive metal oxide samples (Fig. 4) [37].

Self-assembly processes in thin water films

Water-mediated forces play an important role in nanoparticle synthesis and structure formation at the mesoscale [38]. As an example, oriented attachment of nanoparticles represents a key process in the solution-phase growth of hierarchically organized nanostructures. The underlying self-assembly in aqueous dispersions results from the subtle balance between colloidal (i.e., hydration, electrostatic, and dispersion forces) and hydrodynamic forces [38, 39]. Experimentally, oriented attachment of particles in bulk water has been reported for a variety of metal oxides such as TiO_2 [12, 13], ZnO [40], iron oxide, or FeOOH [41]. Complementary molecular dynamics simulations suggest that oriented attachment preferentially involves surfaces that have a higher propensity to hydroxylate and to dissociate water [42]. Therefore, hydroxylation and hydrogen bonding seem to govern particle alignment effects that are followed by coalescence.

Our group recently reported the use of water vapor to induce the self-organization of MgO nanocubes into regularly staggered one-dimensional structures (Fig. 5) [43]. Exposure to water vapor (partial pressure: 30 mbar) and subsequent vacuum annealing at 1173 K results in the reorganization of the MgO nanocubes into one-dimensional structures, that is, MgO nanobars. This transformation evolves via an initial alignment of the MgO cubes [Fig. 5(a)], the formation of intermediate elongated $Mg(OH)_2$ structures, and their reconversion into staggered MgO cube structures by thermal annealing [Fig. 5(c)]. The particles spontaneously orient themselves to form one-dimensional arrays, which, instead of forming perfect stacked cube assemblies, such as observed for metal nanocubes in solution [44], form staggered MgO nanocube assemblies, where the cubes are offset from each other. Ab initio Density Functional Theory (DFT) modelling identifies surface energy changes [Fig. 5(d)] associated with the cube surface hydration and hydroxylation to promote the uncommon staggered assembly of the cubes [43]. This first observation of metal oxide nanoparticle self-organization occurring outside a bulk solution may pave novel routes for inducing texture in ceramics and represents a great test bed for new surface science concepts.

Impact of adsorbed water on materials transformation at elevated temperatures

Thin water films for sintering

Thin water films can also influence sintering processes where a loose metal oxide nanoparticle powder is converted into

https://doi.org/10.1557/jmr.2018.429 Published online by Cambridge University Press

© Materials Research Society 2019

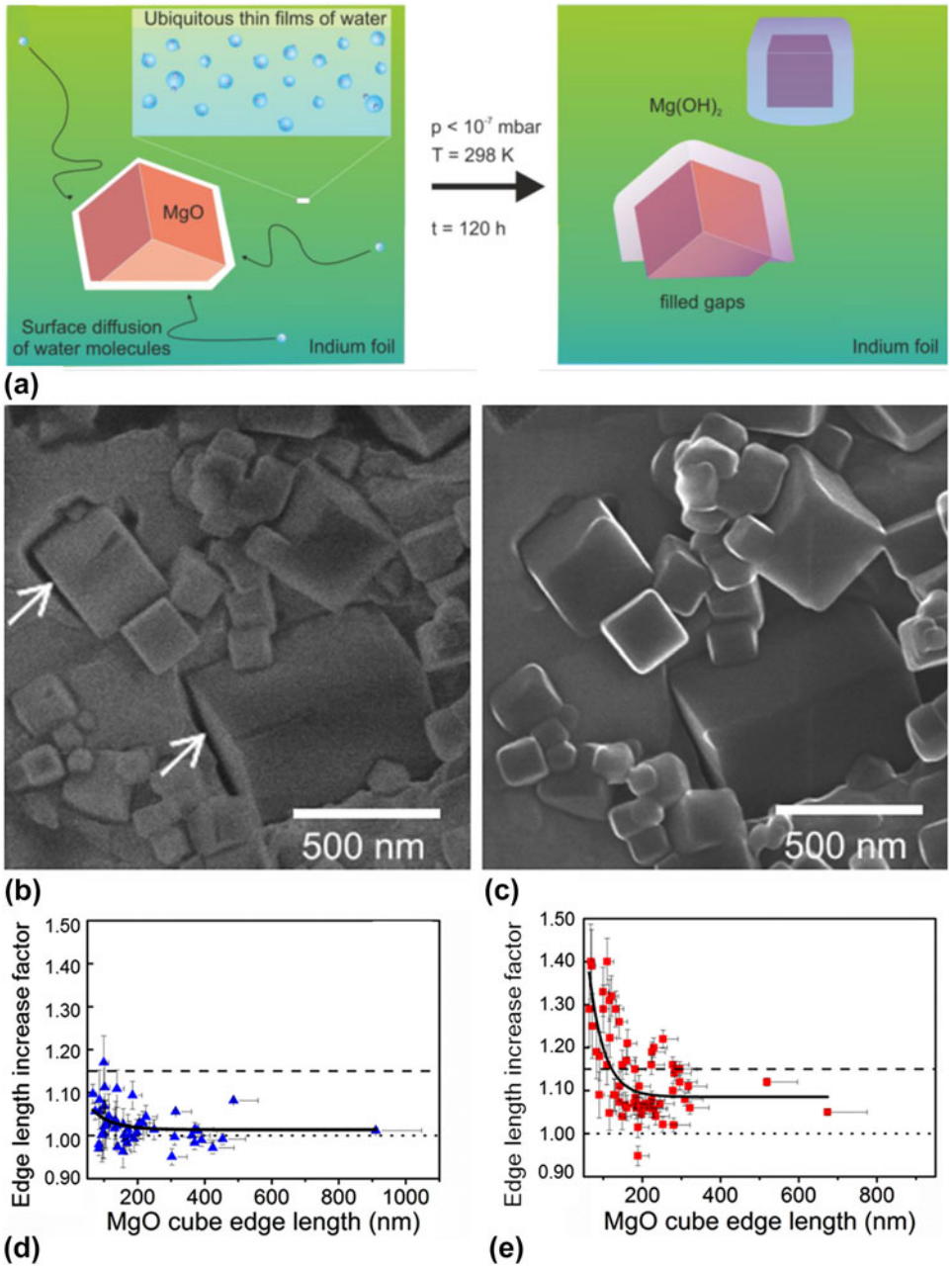


Figure 4: (a) Proposed mechanism of superficial H_2O-induced transformation of MgO cubes into MgO with $Mg(OH)_2$ coatings. This reaction step is associated with characteristic volume expansion effects that are consistent with the observations described above. (b and c) High-magnification HIM images of MgO cubes embedded in an indium foil after 1 h (b), and 4 days in the HIM chamber at a chamber pressure $P < 3 \times 10^{-7}$ mbar (c). Significant volume increase, rounding of the edges, and partial fusion of the particles were observed (see arrows in micrographs). (d and e) Curves showing the edge length increase factor of MgO cubes (L_2/L_1) as a function of the edge length L_1, where L_1 and L_2 are the edge lengths before and after 4 days storage in the vacuum chamber of the HIM, respectively. (d) The indium foil was dried under vacuum before being used as a substrate. (e) The indium foil was used without any further treatment. The dashed line corresponds to a full transformation of MgO into $Mg(OH)_2$ (i.e., $L_2/L_1 = 1.15$). The dotted line corresponds to zero expansion ($L_2/L_1 = 1$). Adapted from Ref. 36.

a dense nanocrystalline material. Sintering is crucial in ceramics processing [45, 46, 47] and can be used to consolidate metal oxide nanoparticle systems with enhanced physicochemical properties [48, 49]. It is a surface elimination process that starts with an assembly of particles in close contact. The initial interfaces or interfacial spots range from point of contact to highly deformed interfaces. With sintering, the contacts grow in size and there is extensive loss of surface area in the initial stage [45, 50]. The determining role of interfacial energies with regard to the densification of consolidated particle systems is well accepted [50, 51]. Since a new type of interface is being created during neck

https://doi.org/10.1557/jmr.2018.429 Published online by Cambridge University Press

© Materials Research Society 2019

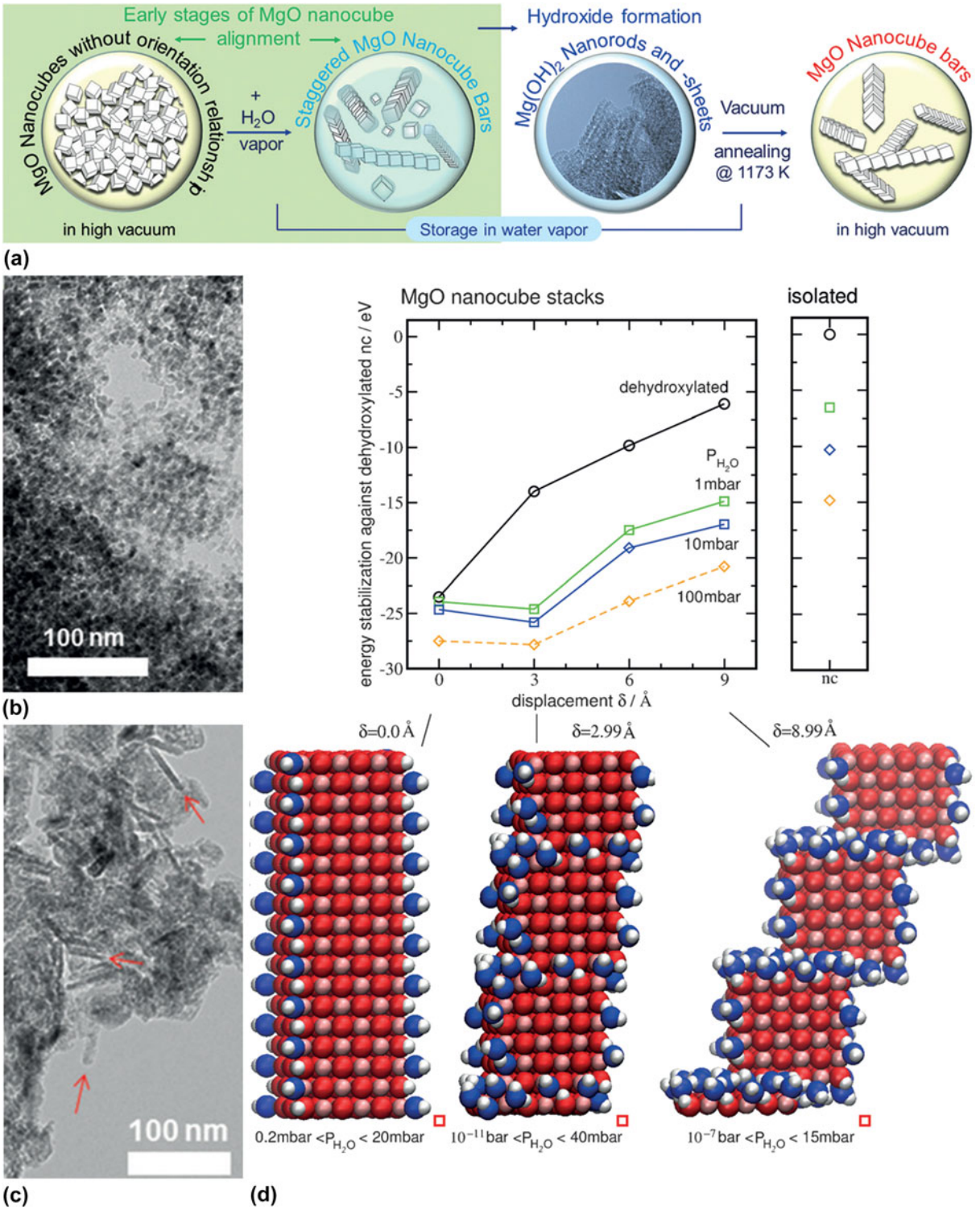


Figure 5: (a) Illustration of water adsorption–induced arrangement of MgO nanocubes into nanobars. (b and c) TEM micrographs of the MgO nanocubes before (b) and after hydroxylation and and dehydroxylation (c), where the arrows indicate the experimentally observed MgO nanocube bars. (d) Stabilization energy of the hydroxylated stacks relative to the dehydroxylated nanocube versus displacement δ along the surface diagonal for different water pressures at $T = 300$ K. Bottom: Geometries of the hydroxylated straight and displaced stacks—oxygen ions are red spheres and magnesium ions are light red spheres. Oxygen ions bound in OH groups or in water are blue spheres and hydrogen atoms are white spheres. The hydroxylated nanocube stacks are stable within the range of water vapor partial pressure indicated below the geometries. Adapted from Ref. 43.

https://doi.org/10.1557/jmr.2018.429 Published online by Cambridge University Press

© Materials Research Society 2019

formation, sintering has an energy cost that is proportional to the grain boundary energy [32, 45, 52]. It was recently found that water adsorbed from ambient on MgO crystalline nanocubes (4 nm) can significantly affect their morphology during vacuum annealing depending on the reactor pressure (Fig. 6). While dynamic vacuum annealing at 1173 K (continuous pumping at pressure $<10^{-5}$ mbar during annealing) does not affect the particle size and shape [Fig. 6(a)], semi-dynamic annealing [Fig. 6(b)], where dynamic pumping is replaced with a constant static O_2 pressure, at $T = 373$ K leads to larger cubic particles (size ranging from 4 nm to ~15 nm) with rounded edge features. The latter phenomenon is due to the increased abundance of step edges that are quite different from the clear-cut sharp edges specific to the parent 4 nm MgO cubes typically obtained from annealing in dynamic vacuum. Annealing at a constant O_2 pressure and without continuous removal of water molecules leads to a significant change in morphology of the particles that become facetted and show significant particle fusion [Fig. 6(c)]. These experiments show that adsorbed water can lead to significant coarsening of the particles. The changes are attributed to enhanced mass transport in the thin water film that acts as a two-dimensional solvent for Mg^{2+} hydration and transport, promoting particle sintering and coarsening at high temperatures.

Instead of using high temperatures and residual water to sinter hydroxylated metal oxide particles, thin water films can also be used to promote the low-temperature sintering of TiO_2 nanoparticles and prepare conducting nanocrystalline TiO_2 films. Such films are of great importance due to their uses in many technological applications such as solar cells, photoelectrodes, photocatalysts, and gas sensors [54, 55]. They are usually prepared via high-temperature sintering, typically performed at 450 °C, and are thus not compatible with the use of heat-sensitive substrates such as flexible polymeric films.

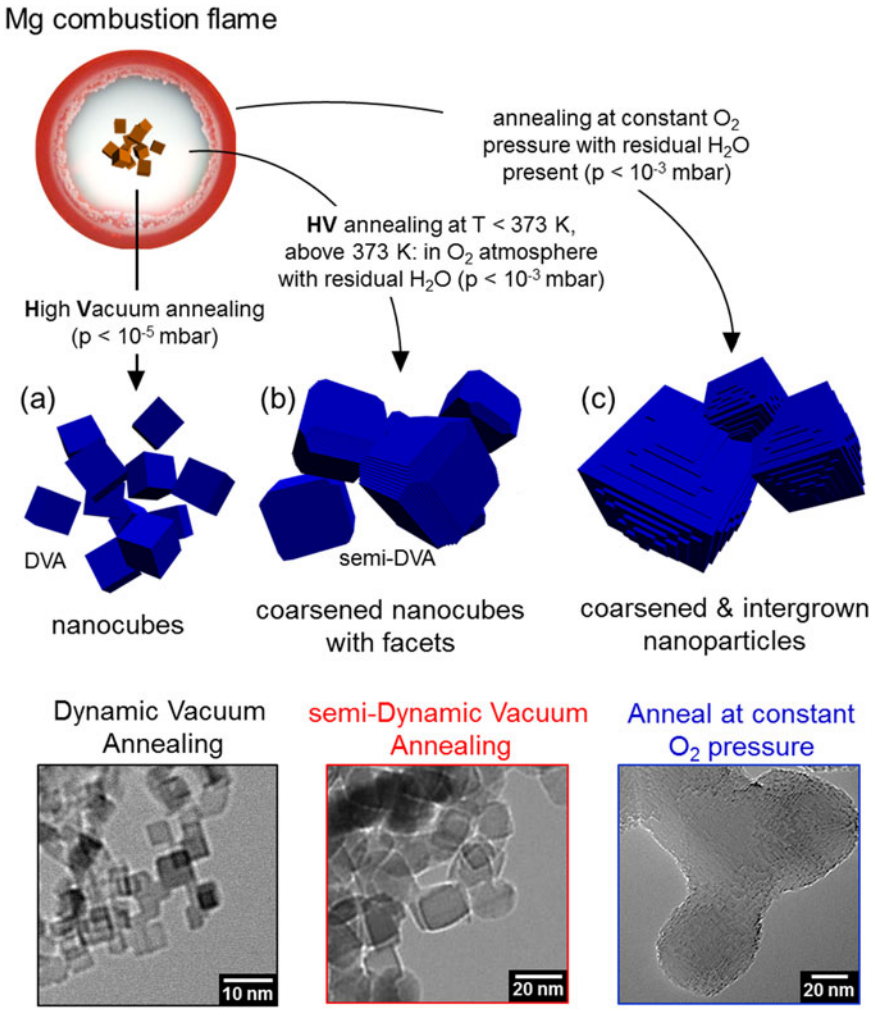


Figure 6: Schematic representation of how different annealing protocols affect the growth of MgO nanocubes synthesized in the Mg combustion flame. Adapted with permission from Ref. 53 (Copyright 2018 WILEY VCH). DVA stands for dynamic vacuum annealing and indicates that annealing was performed under dynamic pumping with a base pressure of $p < 10^{-5}$ mbar.

https://doi.org/10.1557/jmr.2018.429 Published online by Cambridge University Press

© Materials Research Society 2019

Annealing a mixture of TiO_2 nanoparticles with Ti(IV) precursors such as titanium tetraisopropoxide [$Ti(O^iPr)_4$] in water vapor at 100 °C was found to be an efficient route for the preparation of conducting crystalline porous TiO_2 with enhanced photoelectrochemical properties (Fig. 7). While annealing ethanolic solution of $Ti(O^iPr)_4$ under dry conditions at 100 °C yields an amorphous solid, annealing under water vapor at 100 °C yields rutile [Fig. 7(b)]. By using different titanium precursors, it is possible to obtain either rutile or anatase. Such a report shows the beneficial influence of water thin films in the consolidation and preparation of functional ceramics and represents an alternative to high-temperature annealing that is usually necessary for these materials.

Water-assisted crystallization

In addition to promoting sintering, water thin films can also be used to crystallize amorphous metal oxide substrates via dissolution/precipitation processes. For example, some groups have reported on the use of water vapor to crystallize anodized amorphous TiO_2 nanotubes into anatase at moderate temperatures (i.e., lower than 100 °C) [57]. The anodic oxidation of Ti foil into TiO_2 nanotubes has led to a vast field of research [58]. Unfortunately, the as-produced TiO_2 structures after anodization are amorphous and need an additional annealing step in order to be used as functional TiO_2 photocatalysts, typically done at temperatures around 450 °C. Instead of using thermal energy only to crystallize TiO_2, Lamberti et al. [57] recently reported that incubation of amorphous anodized TiO_2 nanotubes for 30 min in water vapor at 90 °C converts amorphous TiO_2 into anatase (Fig. 8). Although at present the mechanism is unclear, a dissolution precipitation reaction is expected to occur due to the changes in the TiO_2 structure morphology that was observed. It is likely that a thin water film hydroxylates the TiO_2 surface, similarly to what occurs at room temperature on MgO surfaces. Dissolution of the Ti(III/IV) species as $[Ti(OH)_6]^{2-}$ in the water film then leads to a supersaturated solution [Eq. (1)], eventually yielding crystallization of anatase via a sequential dehydration step [Eq. (2)] [59].

$$TiO_x + 4H_2O + \left(1 - \frac{x}{2}\right)O_2 \rightarrow Ti(OH)_6^{2-} + 2H^+ (1 < x \leq 2) \quad , \tag{1}$$

$$Ti(OH)_6^{2-} + 2H^+ \rightarrow TiO_2 + 4H_2O \quad . \tag{2}$$

A significant change in the amorphous TiO_2 tubular morphology was observed during water vapor annealing, which was converted into solid anatase wires [57]. This is quite different from what occurs during annealing in liquid water at 90 °C, where the smooth amorphous TiO_2 tube surface is instead replaced with a rough polycrystalline surface composed of granular anatase nanoparticles [Fig. 8(f)] [60]. As expected, the photocatalytic activity of the water vapor–crystallized TiO_2 substrate was much higher than that of the as-synthesized amorphous TiO_2 nanotubes, as shown by the higher decomposition rate of methylene blue under UV illumination of the crystallized TiO_2 substrate [57]. It is interesting to note that the substrates crystallized in water vapor were also slightly more photoactive than the TiO_2 tubes annealed at 450 °C under dry conditions. This is also consistent with a previous work showing that annealing similar TiO_2 nanotubes under water vapor in an autoclave at 180 °C yielded a much higher photoelectrochemical activity than the same substrate annealed at 180 °C and atmospheric pressure (10 times increase in the photocurrent under similar conditions) [61].

Metal oxide immersion into condensed water

Bulk and thin water films can induce strong changes in the composition, structure, and microstructure of both isolated and

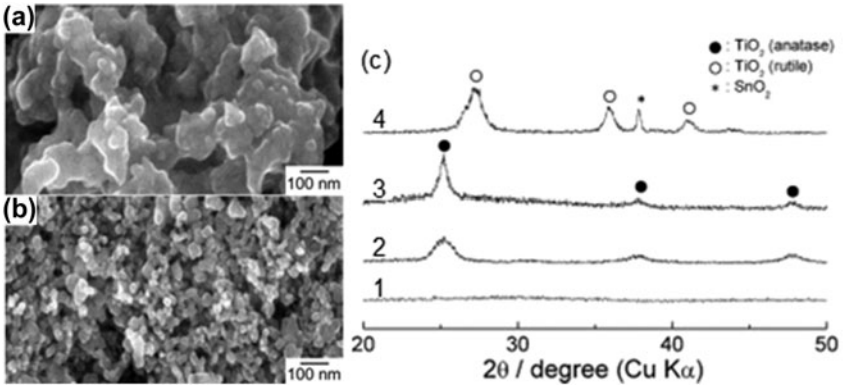


Figure 7: (a and b) SEM photographs of the TiO_2 films produced by mixing P25 particles and $Ti(O^iPr)_4$ before (a) and after annealing in water vapor at 100 °C (b). The undefined matrix seen in (a) is the amorphous $Ti(O^iPr)_4$ film that embeds the TiO_2 particles within. After sintering/crystallization, one can clearly see the TiO_2 crystalline particles. (c) X-ray diffraction (XRD) patterns of the films prepared by heating a solution of at 100 °C for 12 h in a dry oven (1) or by treating the following chemicals in water vapor at 100 °C for 12 h: $Ti(O^iPr)_4$ (2), $TiOSO_4$ (3), and $TiCl_4$ (4). Adapted with permission from Ref. 56 (Copyright 2003 WILEY VCH).

https://doi.org/10.1557/jmr.2018.429 Published online by Cambridge University Press

© Materials Research Society 2019

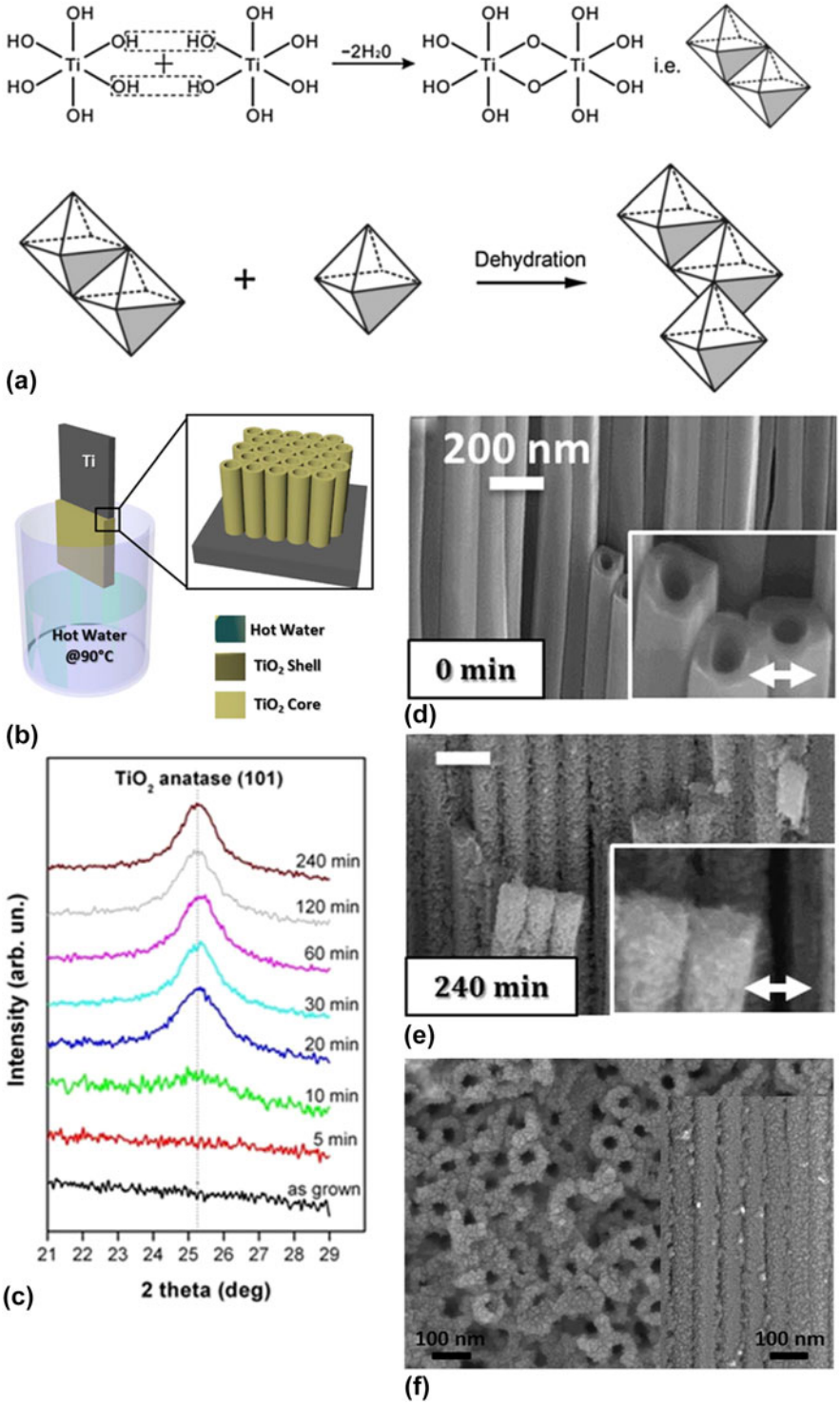


Figure 8: (a) Proposed crystallization mechanism from hydroxylated TiO_2. From Ref. 62. (b) Scheme of the experimental setup used for the crystallization of the amorphous TiO_2 nanotubes in water vapor. (c) X-ray diffraction (XRD) data showing the evolution of the main anatase X-ray diffraction peak [(101) crystal face] during the water vapor exposure. (d and e) SEM images of the TiO_2 tubes before (d) and after 240 min of water vapor annealing at 90 °C (e). (b–e) Adapted with permission from Ref. 57. (f) SEM image of the TiO_2 tubes after 240 min annealing at 90 °C in liquid water. Adapted with permission from Ref. 60 (Copyright 2013 Elsevier).

ensembles of metal oxide nanostructures. While thin water films confine these transformations by limiting mass transport and favoring precipitation at the oxide surface, liquid water usually promotes dissolution/precipitation into bulk water. For example, while MgO particles tend to form core shell structures in the presence of thin water films under high vacuum

https://doi.org/10.1557/jmr.2018.429 Published online by Cambridge University Press

© Materials Research Society 2019

conditions due to partial hydroxylation, they tend to partially or even completely dissolve in liquid water. Figure 9 shows HIM images of MgO micro- and nanocubes pressed onto an In foil and imaged at two different locations before and after being in contact with a water droplet for 17 h. While large microcubes show an increase in particle size due to partial hydroxylation (spot 1), the smallest MgO cubes (spot 2) completely dissolve and precipitate as brucite nanosheets [$Mg(OH)_2$]. Due to the mass transport limitation imposed by the limited thickness of water thin films, such a situation does not occur when the same MgO cubes react with environmental adsorbed water (Fig. 4).

It is interesting to note that the dissolution behavior in liquid water is significantly affected by the structure size: MgO microcubes were found to dissolve much slower than MgO nanocubes (4 nm edge length). It was proposed that the $Mg(OH)_2$ passivation layer grown at the MgO nanocube surface [32] due to the presence of water molecules is not thick enough to influence their dissolution rate, leading to fast and complete dissolution. The situation changes for MgO microcubes whose dimensions allow for the growth of a thick brucite passivating layer [5] that can significantly slow down the dissolution, explaining the different dissolution rate observed for micro- and nanocubes (Fig. 10). Analysis of the dissolution products as a function of time shows that the dissolution rate constant is one order of magnitude higher in the case of the nanocubes [with $k_{Diss} = 3.6 \times 10^{-6}$ mol/(m^2 s)] and is not due to an increase in surface area. Such observations demonstrate that the stability of metal oxide nanostructures in liquid water can be strongly affected by their sizes [24].

These experiments illustrate the difference in complexity between water thin films and bulk water: water thin films on metal oxides are quite well defined due to the limited number of water molecule layers that can be condensed at the substrate surface, while metal oxides immersed in liquid water are much more complex systems. We believe that water thin films on metal oxides are a great test bed to understand and study the interaction between molecular water and metal oxide nanostructures.

Concluding remarks and perspectives

Water adsorption on oxide nanomaterials plays an important but so far underestimated role in materials chemistry and related characterization approaches. For materials synthesis under nonaqueous conditions, the unintended presence of spurious amounts of water may lead to surfactant effects that influence morphology evolution via the stabilization of specific crystal faces. An important example is the stabilization of polar (111) surfaces [11, 63, 64] where surface hydroxylation compensates for surface dipole formation and therefore eliminates the energetic reasons for the instability of corresponding

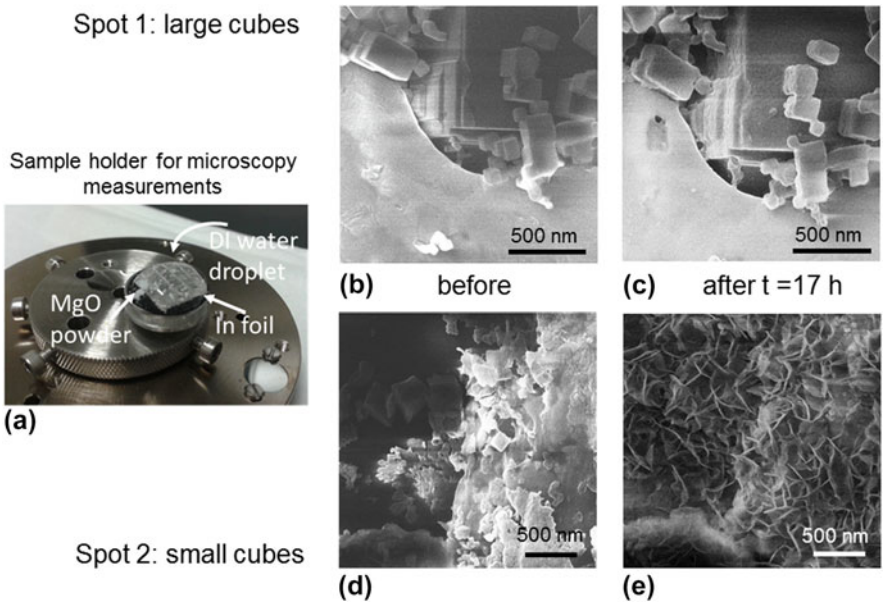


Figure 9: Effect of liquid water on the microstructure of MgO cube and nanocube powders. The HIM images of MgO cubes were taken from one and the same sample (a) on two different areas labelled spot 1 (b, c) and spot 2 (d, e), before (b, d) and after (c, e) exposure to a droplet of liquid water. Clearly, different types of nanostructures can result from the interaction of MgO particle surfaces with H_2O depending on their size and distribution at the sample surface. Comparison of (b) and (c) points to the volume expansion during hydration and hydroxylation, while (d) and (e) reveal that the substantially smaller sized MgO cubes (d) have undergone a dissolution and $Mg(OH)_2$ precipitation mechanism (e), as shown by the formation of network of brucite sheets after exposure to liquid water. Adapted from Ref. 36.

https://doi.org/10.1557/jmr.2018.429 Published online by Cambridge University Press

© Materials Research Society 2019

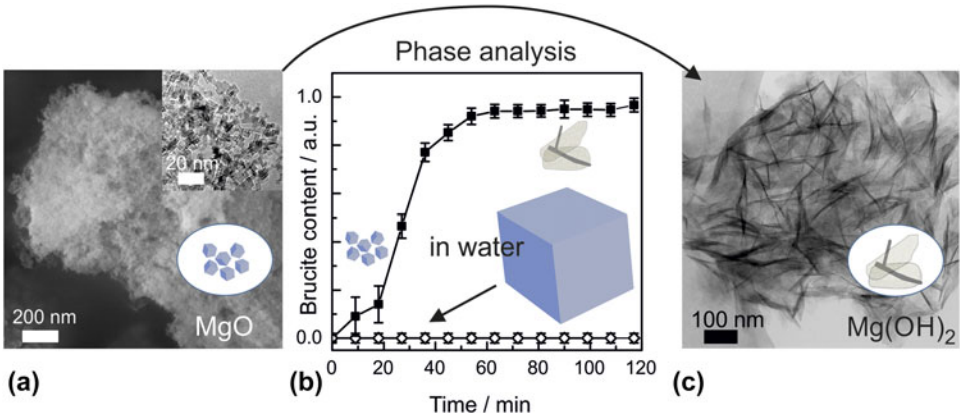


Figure 10: (a and c) Electron microscopy images of native MgO nanocubes (a), and after complete transformation into $Mg(OH)_2$ nanosheets (c). (b) Size-dependent dissolution of MgO nanocubes (top curve) and MgO microcubes (bottom curve) in liquid water. Adapted with permission from Ref. 21 (Copyright (2015) American Chemical Society).

faces. This provides an important handle to tune both the adsorption properties and the catalytic activity of metal oxide surfaces using surface hydroxyls as ubiquitous but—at the same time—structure-directing ligands [64].

Moreover, the fact that high surface area materials can adsorb substantial amounts of water from the ambient atmosphere has a key influence on particle growth and structural reorganization during subsequent thermal processing and sintering [45, 65]. Adsorption-induced changes in the hierarchy of surface energies [53, 66, 67] lead to substantially different particle habits as compared with oxide nanoparticles with bare and dehydroxylated surfaces that are processed under dry vacuum conditions [53]. Apart from the hydroxylation-induced energetic stabilization of specific surface planes that determine the evolution of different crystal shapes [68, 69], thin water films provide a so far unnoticed solvent and reaction medium that converts metastable nanomaterials into new structures at room temperature and at different length scales [70]. This is reminiscent of mineral-based binders where hydration reactions at ambient conditions provide materials of sufficient strength and stability to be used in construction applications.

In this short review, we highlighted water-induced chemical and/or structural changes that are mediated by water vapor and resulting thin films of adsorbed water on MgO and TiO_2 nanostructures. Both metal oxides are canonical model compounds. At the same time, their chemical bondings show characteristic differences with regard to their degree of covalency/ionicity. This determines their interaction with water and their stability in aqueous environments. Being pH dependent, the solubility values of metal oxides range from moderate (>80 mg/L for MgO at pH = 7) to practically insoluble (0.15 mg/L for TiO_2, at pH = 7) [71]. Additionally, variations in particle size, crystal modification, resulting surface terminations and particle shape, pH-dependent surface charges [72], and—last but not least—nature and abundance of reactive surface defects determine the overall particle stability in aqueous environments. Considering the variations in surface reactivity between metal oxide nanocrystals of different composition and synthetic origin, there may exist different mechanistic pathways for water adsorption–induced particle organization and aggregation. However, one can expect the resulting particle-based architectures to have a more characteristic structure at the mesoscale when the individual nanocrystals are facetted and exhibit anisotropic crystal habits [38, 42, 43]. Further experimental and theoretical efforts are needed to explore this exciting playground of mesostructure formation in gaseous or thin liquid film environments that are different from bulk water [14, 38].

The investigation of metal oxide particle surfaces at ambient relative humidity has continuously benefited from the development of experimental techniques in the field of surface science [5, 6, 37, 73, 74], where the interest in solid–liquid interfaces has grown over the last decades. Moreover, the increasing availability of environmental electron microscopy techniques [22, 75, 76] will provide access to complementary information not only to study purely water-induced transformation effects of metal oxide nanomaterials but also to identify surface adsorbed water as a source of experimental artifacts [36, 37].

Acknowledgments

Financial support of the Austrian Science Fund FWF for project P-28797 “Intergranular regions in nanocrystalline ceramics” is gratefully acknowledged. Partial support comes from the University of Salzburg within the Allergy Cancer BioNano (ACBN) Research initiative.

https://doi.org/10.1557/jmr.2018.429 Published online by Cambridge University Press

© Materials Research Society 2019

References

1. **S. Garde and M.L. Schlossman**: Water at functional interfaces. *MRS Bull.* **39**, 1051–1053 (2014).
2. **W. Stumm, L. Sigg, and B. Sulzberger**: *Chemistry of the Solid-Water Interface: Processes at the Mineral-Water and Particle-Water in Natural Systems* (Wiley, New York, 1992).
3. **A. Verdaguer, G.M. Sacha, H. Bluhm, and M. Salmeron**: Molecular structure of water at interfaces: Wetting at the nanometer scale. *Chem. Rev.* **106**, 1478–1510 (2006).
4. **G.E. Ewing**: Ambient thin film water on insulator surfaces. *Chem. Rev.* **106**, 1511–1526 (2006).
5. **F. Ringleb, M. Sterrer, and H-J. Freund**: Preparation of Pd–MgO model catalysts by deposition of Pd from aqueous precursor solutions onto Ag(001)-supported MgO(001) thin films. *Appl. Catal., A* **474**, 186–193 (2014).
6. **O. Bjorneholm, M.H. Hansen, A. Hodgson, L-M. Liu, D. T. Limmer, A. Michaelides, P. Pedevilla, J. Rossmeisl, H. Shen, G. Tocci, E. Tyrode, M-M. Walz, J. Werner, and H. Bluhm**: Water at interfaces. *Chem. Rev.* **116**, 7698–7726 (2016).
7. **M.E. McBriarty, G.F. von Rudorff, J.E. Stubbs, P.J. Eng, J. Blumberger, and K.M. Rosso**: Dynamic stabilization of metal oxide-water interfaces. *J. Am. Chem. Soc.* **139**, 2581–2584 (2017).
8. **R. Mu, Z-J. Zhao, Z. Dohnálek, and J. Gong**: Structural motifs of water on metal oxide surfaces. *Chem. Soc. Rev.* **46**, 1785–1806 (2017).
9. **M. Sterrer, N. Nilius, S. Shaikhutdinov, M. Heyde, T. Schmidt, and H-J. Freund**: Interaction of water with oxide thin film model systems. *J. Mater. Res.* FirstView online at https://doi.org/10.1557/jmr.2018.454 (2019).
10. **J. Goniakowski, F. Finocchi, and C. Noguera**: Polarity of oxide surfaces and nanostructures. *Rep. Prog. Phys.* **71**, 16501 (2008).
11. **C. Noguera and J. Goniakowski**: Polarity in oxide nano-objects. *Chem. Rev.* **113**, 4073–4105 (2013).
12. **M. Niederberger and H. Cölfen**: Oriented attachment and mesocrystals: Non-classical crystallization mechanisms based on nanoparticle assembly. *Phys. Chem. Chem. Phys.* **8**, 3271–3287 (2006).
13. **H. Cölfen and M. Antonietti**: *Mesocrystals and Nonclassical Crystallization* (Wiley, Chichester, England, Hoboken, New Jersey, 2008).
14. **X. Zhang, Z. Shen, J. Liu, S.N. Kerisit, M.E. Bowden, M. L. Sushko, J.J. de Yoreo, and K.M. Rosso**: Direction-specific interaction forces underlying zinc oxide crystal growth by oriented attachment. *Nat. Commun.* **8**, 835 (2017).
15. **G. Spoto, E.N. Gribov, G. Ricchiardi, A. Damin, D. Scarano, S. Bordiga, C. Lamberti, and A. Zecchina**: Carbon monoxide MgO from dispersed solids to single crystals: A review and new advances. *Prog. Surf. Sci.* **76**, 71–146 (2004).
16. **U. Diebold, S-C. Li, and M. Schmid**: Oxide surface science. *Annu. Rev. Phys. Chem.* **61**, 129–148 (2010).
17. **L.E. Erickson, R.T. Koodali, and R.M. Richards**: *Nanoscale Materials in Chemistry: Environmental Applications* (American Chemical Society, Washington, 2010).
18. **T. Berger and O. Diwald:** *Chapter 9: Defects in Metal Oxide Nanoparticle Powders*: In *Defects at Oxide Surfaces*, J. Jupille and G. Thornton, 273–302 eds. (Springer International Publishing, Switzerland, 2015).
19. **M. Sterrer, T. Berger, O. Diwald, E. Knözinger, P.V. Sushko, and A.L. Shluger**: Chemistry at corners and edges: Generation and adsorption of H atoms on the surface of MgO nanocubes. *J. Chem. Phys.* **123**, 064714 (2005).
20. **J. Schneider, M. Franke, M. Gurrath, M. Röckert, T. Berger, J. Bernardi, B. Meyer, H-P. Steinrück, O. Lytken, and O. Diwald**: Porphyrin metalation at MgO surfaces: A spectroscopic and quantum mechanical study on complementary model systems. *Chem.-Eur. J.* **22**, 1744–1749 (2016).
21. **I.S. Altman, I.E. Agranovski, and M. Choi**: On nanoparticle surface growth: MgO nanoparticle formation during a Mg particle combustion. *Appl. Phys. Lett.* **84**, 5130–5132 (2004).
22. **M. Gajdardziska-Josifovska and R. Sharma**: Interaction of oxide surfaces with water: Environmental transmission electron microscopy of MgO hydroxylation. *Microsc. Microanal.* **11**, 524–533 (2005).
23. **D. Scarano, S. Bertarione, F. Cesano, G. Spoto, and A. Zecchina**: Imaging polycrystalline and smoke MgO surfaces with atomic force microscopy: A case study of high resolution image on a polycrystalline oxide. *Surf. Sci.* **570**, 155–166 (2004).
24. **S.O. Baumann, J. Schneider, A. Sternig, D. Thomele, S. Stankic, T. Berger, H. Grönbeck, and O. Diwald**: Size effects in MgO cube dissolution. *Langmuir* **31**, 2770–2776 (2015).
25. **N. Siedl, D. Koller, A.K. Sternig, D. Thomele, and O. Diwald**: Photoluminescence quenching in compressed MgO nanoparticle systems. *Phys. Chem. Chem. Phys.* **16**, 8339–8345 (2014).
26. **M.J. Elser, T. Berger, D. Brandhuber, J. Bernardi, O. Diwald, and E. Knözinger**: Particles coming together: Electron centers in adjoined TiO_2 nanocrystals. *J. Phys. Chem. B* **110**, 7605–7608 (2006).
27. **S.O. Baumann, M.J. Elser, M. Auer, J. Bernardi, N. Hüsing, and O. Diwald**: Solid-solid interface formation in TiO_2 nanoparticle networks. *Langmuir* **27**, 1946–1953 (2011).
28. **M. Foster, M. D'Agostino, and D. Passno**: Water on MgO(100)—An infrared study at ambient temperatures. *Surf. Sci.* **590**, 31–41 (2005).
29. **P. Fenter and S.S. Lee**: Hydration layer structure at solid–water interfaces. *MRS Bull.* **39**, 1056–1061 (2014).
30. **Z. Zhang, P. Fenter, L. Cheng, N.C. Sturchio, M.J. Bedzyk, M. Předota, A. Bandura, J.D. Kubicki, S.N. Lvov, P. T. Cummings, A.A. Chialvo, M.K. Ridley, P. Bénézeth, L. Anovitz, D.A. Palmer, M.L. Machesky, and D. J. Wesolowski**: Ion adsorption at the rutile–water interface: Linking molecular and macroscopic properties. *Langmuir* **20**, 4954–4969 (2004).
31. **A. Sternig, D. Koller, N. Siedl, O. Diwald, and K. McKenna**: Exciton formation at solid-solid interfaces: A systematic

https://doi.org/10.1557/jmr.2018.429 Published online by Cambridge University Press

© Materials Research Society 2019

experimental and ab initio study on compressed MgO nanopowders. *J. Phys. Chem. A* **116**, 10103–10112 (2012).

32. **S. Hayun, T. Tran, S.V. Ushakov, A.M. Thron, K. van Benthem, A. Navrotsky, and R.H.R. Castro**: Experimental methodologies for assessing the surface energy of highly hygroscopic materials: The case of nanocrystalline magnesia. *J. Phys. Chem. C* **115**, 23929–23935 (2011).
33. **M.D. Susman, H.N. Pham, A.K. Datye, S. Chinta, and J.D. Rimer**: Factors governing MgO(111) Faceting in the thermal decomposition of oxide precursors. *Chem. Mater.* **30**, 2641–2650 (2018).
34. **R.A. van Santen**: *Modern Heterogeneous Catalysis: An Introduction* (Wiley-VCH, Verlag GmbH & Co. KGaA, Weinheim, Germany, 2017).
35. **A.G. Gheisi, A.K. Sternig, G. Redhammer, and O. Diwald**: Thin water films and magnesium hydroxide fiber growth. *RSC Adv.* **5**, 82564–82569 (2015).
36. **R. Schwaiger, J. Schneider, G.R. Bourret, and O. Diwald**: Hydration of magnesia cubes: A helium ion microscopy study. *Beilstein J. Nanotechnol.* **7**, 302–309 (2016).
37. **D.R. Baer, M.H. Engelhard, G.E. Johnson, J. Laskin, J. Lai, K. Mueller, P. Munusamy, S. Thevuthasan, H. Wang, N. Washton, A. Elder, B.L. Baisch, A. Karakoti, S.V.N. T. Kuchibhatla, and D. Moon**: Surface characterization of nanomaterials and nanoparticles: Important needs and challenging opportunities. *J. Vac. Sci. Technol., A* **31**, 50820 (2013).
38. **Z. Shen, J. Chun, K.M. Rosso, and C.J. Mundy**: Surface chemistry affects the efficacy of the hydration force between two ZnO$(10\bar{1}\bar{0})$ surfaces. *J. Phys. Chem. C* **122**, 12259–12266 (2018).
39. **D.A. Welch, T.J. Woehl, C. Park, R. Faller, J.E. Evans, and N. D. Browning**: Understanding the role of solvation forces on the preferential attachment of nanoparticles in liquid. *ACS Nano* **10**, 181–187 (2016).
40. **D. Li, M.H. Nielsen, J.R.I. Lee, C. Frandsen, J.F. Banfield, and J. J. De Yoreo**: Direction-specific interactions control crystal growth by oriented attachment. *Science* **336**, 1014–1018 (2012).
41. **J.A. Soltis and R.L. Penn**: *Chapter 11: Oriented Attachment and Nonclassical Formation in Iron Oxides,* from *Iron Oxides: From Nature to Applications*, 243–267 (Wiley-VCH Verlag GmbH & Co KGa, 2016, Boschstr. 12, 69469, Weinheim Germany.).
42. **M. Raju, A.C.T. van Duin, and K.A. Fichthorn**: Mechanisms of oriented attachment of TiO_2 nanocrystals in vacuum and humid environments: Reactive molecular dynamics. *Nano Lett.* **14**, 1836–1842 (2014).
43. **D. Thomele, G.R. Bourret, J. Bernardi, M. Bockstedte, and O. Diwald**: Hydroxylation induced alignment of metal oxide nanocubes. *Angew. Chem., Int. Ed.* **56**, 1407–1410 (2017).
44. **B. Gao, G. Arya, and A.R. Tao**: Self-orienting nanocubes for the assembly of plasmonic nanojunctions. *Nat. Nanotechnol.* **7**, 433–437 (2012).
45. **R.H.R. Castro, D. Gouvêa, and F. Wakai**: Sintering and nanostability: The thermodynamic perspective. *J. Am. Ceram. Soc.* **99**, 1105–1121 (2016).
46. **A.R. Gheisi, M. Niedermaier, G. Tippelt, W. Lottermoser, J. Bernardi, and O. Diwald**: Iron precursor decomposition in the magnesium combustion flame: A new approach for the synthesis of particulate metal oxide nanocomposites. *Part. Part. Syst. Charact.* **34**, 1700109 (2017).
47. **R.K. Bordia, S-J.L. Kang, and E.A. Olevsky**: Current understanding and future research directions at the onset of the next century of sintering science and technology. *J. Am. Ceram. Soc.* **100**, 2314–2352 (2017).
48. **K. Lu**: Sintering of nanoceramics. *Int. Mater. Rev.* **53**, 21–38 (2008).
49. **K. Lu**: *Nanoparticulate Materials* (John Wiley & Sons, Inc., Hoboken, New Jersey, 2012).
50. **S. Phokha, J. Klinkaewnarong, S. Hunpratub, K. Boonserm, E. Swatsitang, and S. Maensiri**: Ferromagnetism in Fe-doped MgO nanoparticles. *J. Mater. Sci.: Mater. Electron.* **27**, 33–39 (2016).
51. **W. Folly, S. Soriano, J.P. Sinnecker, and M.A. Novak**: Dynamic behavior of superparamagnetic iso-oriented magnesioferrite nanoparticles. *Phys. B* **384**, 300–302 (2006).
52. **R.H.R. Castro, R.B. Tôrres, G.J. Pereira, and D. Gouvêa**: Interface energy measurement of MgO and ZnO: Understanding the thermodynamic stability of nanoparticles. *Chem. Mater.* **22**, 2502–2509 (2010).
53. **D. Thomele, A.R. Gheisi, M. Niedermaier, M.S. Elsässer, J. Bernardi, H. Grönbeck, and O. Diwald**: Thin water films and particle morphology evolution in nanocrystalline MgO. *J. Am. Ceram. Soc.* **116**, 7698 (2018).
54. **T. Berger, D. Monllor-Satoca, M. Jankulovska, T. Lana-Villarreal, and R. Gómez**: The electrochemistry of nanostructured titanium dioxide electrodes. *ChemPhysChem* **13**, 2824–2875 (2012).
55. **L. Sun, A.A. Haidry, Q. Fatima, Z. Li, and Z. Yao**: Improving the humidity sensing below 30% RH of TiO_2 with GO modification. *Mater. Res. Bull.* **99**, 124–131 (2018).
56. **D. Zhang, T. Yoshida, and H. Minoura**: Low-temperature fabrication of efficient porous titania photoelectrodes by hydrothermal crystallization at the solid/gas interface. *Adv. Mater.* **15**, 814–817 (2003).
57. **A. Lamberti, A. Chiodoni, N. Shahzad, S. Bianco, M. Quaglio, and C.F. Pirri**: Ultrafast room-temperature crystallization of TiO_2 nanotubes exploiting water-vapor treatment. *Sci. Rep.* **5**, 7808 (2015).
58. **P. Roy, S. Berger, and P. Schmuki**: TiO_2 nanotubes: Synthesis and applications. *Angew. Chem., Int. Ed.* **50**, 2904–2939 (2011).
59. **K. Huo, H. Wang, X. Zhang, Y. Cao, and P.K. Chu**: Heterostructured TiO_2 nanoparticles/nanotube arrays: In situ formation from amorphous TiO_2 nanotube arrays in water and enhanced photocatalytic activity. *ChemPlusChem* **77**, 323–329 (2012).
60. **W. Krengvirat, S. Sreekantan, A-F. Mohd Noor, N. Negishi, G. Kawamura, H. Muto, and A. Matsuda**: Low-temperature

https://doi.org/10.1557/jmr.2018.429 Published online by Cambridge University Press

© Materials Research Society 2019

crystallization of TiO_2 nanotube arrays via hot water treatment and their photocatalytic properties under visible-light irradiation. *Mater. Chem. Phys.* **137**, 991–998 (2013).

61. **J. Liu, Z. Liu, T. Zhang, J. Zhai, and L. Jiang**: Low-temperature crystallization of anodized TiO_2 nanotubes at the solid-gas interface and their photoelectrochemical properties. *Nanoscale* **5**, 6139–6144 (2013).
62. **Z. Chen and K. Zhou**: Surface morphology, phase structure and property evolution of anodized titanium during water vapor exposure. *Surf. Coat. Technol.* **263**, 61–65 (2015).
63. **J. Hu, K. Zhu, L. Chen, C. Kubel, and R. Richards**: MgO(111) Nanosheets with unusual surface activity. *J. Phys. Chem. C* **111**, 12038–12044 (2007).
64. **C.A. Cadigan, A.R. Corpuz, F. Lin, C.M. Caskey, K.B. H. Finch, X. Wang, and R.M. Richards**: Nanoscale (111) faceted rock-salt metal oxides in catalysis. *Catal. Sci. Technol.* **3**, 900–911 (2013).
65. **K. Lu**: *Nanoparticulate Materials: Synthesis, Characterization, and Processing* (Wiley, Hoboken, New Jersey, 2013).
66. **P. Geysermans, F. Finocchi, J. Goniakowski, R. Hacquart, and J. Jupille**: Combination of (100), (110) and (111) facets in MgO crystals shapes from dry to wet environment. *Phys. Chem. Chem. Phys.* **11**, 2228–2233 (2009).
67. **A. Sternig, S. Klacar, J. Bernardi, M. Stöger-Pollach, H. Grönbeck, and O. Diwald**: Phase separation at the nanoscale: Structural properties of BaO segregates on MgO-based nanoparticles. *J. Phys. Chem. C* **115**, 15853–15861 (2011).
68. **A.S. Barnard**: Modelling of nanoparticles: Approaches to morphology and evolution. *Rep. Prog. Phys.* **73**, 86502 (2010).
69. **H. Guo and A.S. Barnard**: Thermodynamic modelling of nanomorphologies of hematite and goethite. *J. Mater. Chem.* **21**, 11566 (2011).
70. **A. Gheisi, A. Sternig, M. Rangus, G. Redhammer, M. Hartmann, and O. Diwald**: Spontaneous growth of magnesium hydroxide fibers at ambient conditions. *Cryst. Growth Des.* **14**, 4236–4239 (2014).
71. **N.J. Rogers, N.M. Franklin, S.C. Apte, and G.E. Batley**: The importance of physical and chemical characterization in nanoparticle toxicity studies. *Integr. Environ. Assess. Manage.* **3**, 303–304 (2007).
72. **O. Söhnel**: Electrolyte crystal-aqueous solution interfacial tensions from crystallization data. *J. Cryst. Growth* **57**, 101–108 (1982).
73. **W.E. Kaden, S. Pomp, M. Sterrer, and H-J. Freund**: Insights into silica bilayer hydroxylation and dissolution. *Top. Catal.* **60**, 471–480 (2017).
74. **M.A. Brown, A.B. Redondo, M. Sterrer, B. Winter, G. Pacchioni, Z. Abbas, and J.A. van Bokhoven**: Measure of surface potential at the aqueous-oxide nanoparticle interface by XPS from a liquid microjet. *Nano Lett.* **13**, 5403–5407 (2013).
75. **F.F. Tao and P.A. Crozier**: Atomic-scale observations of catalyst structures under reaction conditions and during catalysis. *Chem. Rev.* **116**, 3487–3539 (2016).
76. **F.F. Tao and M. Salmeron**: In situ studies of chemistry and structure of materials in reactive environments. *Science* **331**, 171–174 (2011).

https://doi.org/10.1557/jmr.2018.429 Published online by Cambridge University Press

© Materials Research Society 2019